

Accepted version

Dalius Misiunas, John Vtkovsk, Gustaf Olsson, Angus Simpson, M.ASCE, and Martin Lambert,
Pipeline break detection using pressure transient monitoring
Journal of Water Resources Planning and Management, 2005; 131(4):316-325

©ASCE

[http://doi.org/10.1061/\(ASCE\)0733-9496\(2005\)131:4\(316\)](http://doi.org/10.1061/(ASCE)0733-9496(2005)131:4(316))

Source:

<http://dx.doi.org/10.1061/9780784479018.ch03>

Authors may post the final draft of their work on open, unrestricted Internet sites or deposit it in an institutional repository when the draft contains a link to the bibliographic record of the published version in the ASCE Civil Engineering Database. Final draft means the version submitted to ASCE after peer review and prior to copyediting or other ASCE production activities; it does not include the copyedited version, the page proof, or a PDF of the published version.

February 23, 2015

<http://hdl.handle.net/2440/16741>

Pipeline break detection using the transient monitoring

by

Misiunas, D., Vítkovský, J., Olsson, G., Simpson, A.R. and Lambert, M.F.

Journal of Water Resources Planning and Management

Citation:

Misiunas, D., Vítkovský, J., Olsson, G., Simpson, A.R. and Lambert, M.F. (2005). "Pipeline break detection using the transient monitoring" *Journal of Water Resources Planning and Management*, American Society of Civil Engineers 131(4), July–August, 316–325. (30 citations to Jan. 2013 – Scopus)

For further information about this paper please email Angus Simpson at angus.simpson@adelaide.edu.au

Discrete Blockage Detection in Pipelines Using the Frequency Response Diagram: Numerical Study

Pedro J. Lee¹; John P. Vítkovský²; Martin F. Lambert³; Angus R. Simpson⁴; and James A. Liggett⁵

Abstract: This paper proposes the use of fluid transients as a noninvasive technique for locating blockages in transmission pipelines. By extracting the behavior of the system in the form of a frequency response diagram, discrete blockages within the pipeline were shown to induce an oscillatory pattern on the peaks of this response diagram. This pattern can be related to the location and size of the blockage. A simple analytical expression that can be used to detect, locate, and size discrete blockages is presented, and is shown able to cater for multiple blockages existing simultaneously within the system. The structure of the expression suggests that the proposed technique can be extended to situations where system parameters may not be known to a high accuracy and also to more complex network scenarios, although future studies may be required to verify these possibilities.

DOI: XXXX

CE Database subject headings: Frequency response; Linear systems; Transients; Water pipelines; Resonance; Numerical analysis.

Introduction

The increasing industrial reliance on pipeline systems for the transport of materials has led to the recent emphasis on technologies for the fast detection and location of faults within such systems. Amongst the types of problems that can occur in a pipeline system, the formation of blockages within the pipe poses a most elusive problem for existing fault detection technologies. Unlike leaks within piping systems, a blockage does not generate clear external indicators for its location such as the release and accumulation of fluids around the pipe. Often intrusive procedures, such as the insertion of a closed-circuit camera or a robotic pig, are required to determine the location of blockages. The creation of nonintrusive techniques for fault detection that gives a clear picture of the internal conditions of the pipeline is desirable, and the use of fluid transients for this purpose is a promising development.

Fluid transients are modified by the conditions within the pipeline. The behavior of these transient waves can be used to indicate the internal condition of the pipe system. There has been a range of publications proposing different strategies of fluid transient usage in leak detection and these methods share a common theme in that a small amplitude disturbance—a fluid transient—is injected into a pipe and the subsequent pressure response is measured and analyzed to derive system information. This type of analysis is more commonly known as system response extraction and forms the basis of well-established methodologies used to extract dynamic responses of complex mechanical and electrical systems.

The behavior of any system can be summarized by a frequency response diagram (FRD) that describes how the system affects each individual frequency component of the injected transient signal. Under the influence of transients pipeline systems display near linear behavior and the FRD is defined as

$$H(\omega) = \frac{\mathcal{F}\{y(t)\}}{\mathcal{F}\{x(t)\}} \quad (1)$$

where $H(\omega)$ = frequency response function; \mathcal{F} = Fourier transform of the functions $x(t)$ and $y(t)$, which stand for input and output, respectively (Lynn 1982); ω = frequency; and t = time. The input to the system is given by the nature of the injected transient signal (e.g., the induced discharge variation at the transient generating valve due to the valve movement), and the output is given by the measured head response from the pipe.

The medical field was among the first to use the FRD of pipeline systems for measurement in the human vocal tract (Schroeder 1967; Mermelstein 1967; De Salis and Oldham 2001). These techniques rely on the measured shifts in the resonant frequencies of the pipeline system for the detection of extended blockages within gas transmission pipeline systems. Unless the extent of the blockage is substantial in relation to the scale of the pipeline system, these shifts in the resonant frequencies are often not perceptible in water pipes. For mild blockages in large systems, the blockage can be considered as discrete, similar to that generated by a partially closed inline valve.

¹Lecturer, Dept. of Civil Engineering, College of Engineering, Univ. of Canterbury, Private 4800, Christchurch, 8020, New Zealand. E-mail: Pedro.lee@canterbury.ac.nz

²Hydrologist, Water Assessment Group, Dept. of Natural Resources and Water, Queensland Government, Indooroopilly QLD 4068, Australia. E-mail: john.vitkovsky@nrw.qld.gov.au

³Associate Professor, Centre for Applied Modelling in Water Engineering, School of Civil and Environmental Engineering, Univ. of Adelaide, Adelaide SA 5005, Australia. E-mail: mlambert@civeng.adelaide.edu.au

⁴Professor, Centre for Applied Modelling in Water Engineering, School of Civil and Environmental Engineering, Univ. of Adelaide, Adelaide SA 5005, Australia. E-mail: asimpson@civeng.adelaide.edu.au

⁵Professor Emeritus, School of Civil and Environmental Engineering, Cornell Univ., Ithaca, NY 14853-3501. E-mail: jal8@cornell.edu

Note. Discussion open until October 1, 2008. Separate discussions must be submitted for individual papers. To extend the closing date by one month, a written request must be filed with the ASCE Managing Editor. The manuscript for this paper was submitted for review and possible publication on December 2, 2003; approved on March 12, 2007. This paper is part of the *Journal of Hydraulic Engineering*, Vol. 134, No. 5, May 1, 2008. ©ASCE, ISSN 0733-9429/2008/5-1-XXXX/\$25.00.

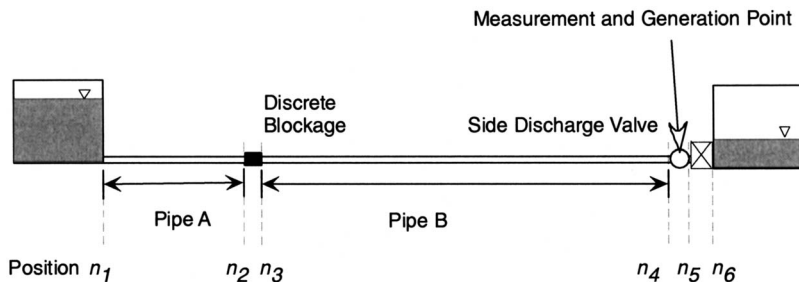


Fig. 1. Pipeline system under consideration

68 There has been recent work into the use of the FRD for de-
 69 tecting blockages in liquid pipelines (Wang et al. 2005; Mohap-
 70 atra et al. 2006; Lee and Vítkovský 2006), but the effect of a
 71 discrete blockage on the FRD has not been quantified. In this
 72 paper an analytical expression is derived that allows discrete
 73 blockages to be detected within a single pipeline system using the
 74 shape of the FRD. In a clear pipeline system without blockages,
 75 the FRD has a series of resonant peaks that decay smoothly with
 76 frequency due to unsteady frictional damping (Vítkovský et al.
 77 2003). A discrete blockage within the system results in an oscil-
 78 latory pattern being imposed on the resonant peak magnitudes.
 79 This is illustrated in a numerical example using the pipeline in
 80 Fig. 1.

81 The numerical example system in Fig. 1 consists of a 2,000 m
 82 length of a 0.3 m diameter pipeline and is bounded by constant
 83 head reservoirs. The heads for the upstream and downstream
 84 reservoirs are 50 and 20 m, respectively. There is a fully opened
 85 inline valve at the downstream end of the system, with a
 86 valve loss coefficient, $C_V=0.002 \text{ m}^{5/2} \text{ s}^{-1}$. The wave speed of
 87 the system is $1,200 \text{ m s}^{-1}$ and the transient is generated by
 88 the perturbation of a side discharge valve located just upstream of
 89 the inline valve. The impedance of the blockage, $I_B=\Delta H_{B0}/Q_{B0}$
 90 $=763.9 \text{ m}^{-2} \text{ s}$ and the dimensionless location of the blockage is
 91 defined as

$$x_b^* = \frac{L_A}{L_A + L_B} \quad (2)$$

92 where L_A, L_B =length of the pipe section A and section B as indi-
 93 cated in Fig. 1. The size of the blockage can be expressed in
 94 dimensionless form as $I_B^*=I_B/B$, where $B=a/gA$ and is the char-

acteristic impedance of the pipe. The dimensionless blockage size 96
 for this case is $I_B^*=0.44$. This blockage size was purposely made 97
 large to clearly shown the impact of a blockage on the FRD. For 98
 the purpose of isolating the impact of the blockage on the FRD, 99
 the pipeline is assumed to be frictionless. The impact of steady 100
 friction reduces the magnitude of the FRD peaks uniformly and 101
 does not change the pattern induced by the blockage on the peaks 102
 in the FRD. The FRD of the system is extracted in Fig. 2, where 103
 Eq. (1) is applied to the resultant transient response. The input 104
 and output from the system are the discharge perturbation gener- 105
 ated by the movement of the side discharge valve located at the 106
 downstream end and the measured head perturbation at the valve 107
 for the duration of the transient signal, respectively (see Fig. 1). 108
 Details concerning the extraction of the FRD can be found in Lee 109
 et al. (2004b, 2005). The FRD of a pipeline system contains a 110
 series of regular harmonic peaks, spaced according to the funda- 111
 mental frequency of the system. Fig. 2 shows that for a blockage- 112
 free system, the magnitudes of the peaks in the FRD are uniform, 113
 whereas a blockage within the system induces a sinusoidal-like 114
 oscillation on the peaks of the FRD. The following section shows 115
 the analytical expression for this oscillation that can be used to 116
 locate the blockage. 117

Impact of Blockage on the Peaks of the FRD 118

Given a pipeline system excited at a particular angular frequency, 119
 ω , the prediction of the head response at any point is given by the 120
 linearized transfer matrix equation (Chaudhry 1987; Wylie and 121
 Streeter 1993). Lee et al. (2005) present analysis relating to the 122

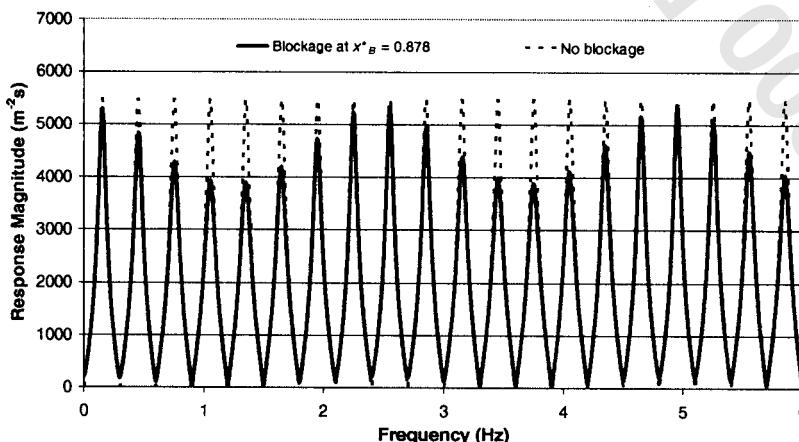


Fig. 2. FRD of the blocked and intact pipeline shown in Fig. 1 generated from the transfer matrices

123 validity of the linear assumption in unsteady pipeline systems.
 124 The transfer matrix method uses a series of individual matrices,
 125 each corresponding to an element within the pipeline system.
 126 These matrices are multiplied in the order of their location start-
 127 ing from the downstream end to produce an overall transfer ma-
 128 trix of the pipe system, U [see Eq. (3)]. Combined with known
 129 boundary conditions, this overall transfer matrix is then solved for
 130 the complex discharge and head perturbations (q and h) at the
 131 extremities of the pipeline. The third row and the third column of
 132 this matrix are included to cater for external head and discharge
 133 perturbations imposed on the system

$$\begin{Bmatrix} q \\ h \\ 1 \end{Bmatrix}^{n_5} = \begin{bmatrix} U_{11} & U_{12} & U_{13} \\ U_{21} & U_{22} & U_{23} \\ U_{31} & U_{32} & U_{33} \end{bmatrix} \begin{Bmatrix} q \\ h \\ 1 \end{Bmatrix}^{n_1} \quad (3)$$

134 where, n_1, n_5 denote the position in the system of Fig. 1;
 135 q, h =discharge and head perturbations; and $U_{ij}=(i, j)$ th entry in
 136 the system transfer matrix, U . Eq. (3), once solved, can be used to
 137 determine the head and discharge perturbations at any point
 138 within the system. Expanding Eq. (3) gives

$$q_{n_5} = U_{11}q_{n_1} + U_{12}h_{n_1} + U_{13} \quad (4)$$

$$h_{n_5} = U_{21}q_{n_1} + U_{22}h_{n_1} + U_{23} \quad (5)$$

142 The orifice equation (in a linearized form) relates the head loss
 143 (ΔH_{V0}) and discharge (Q_{V0}) through the side-discharge valve as

$$h_{n_5} = \frac{2\Delta H_{V0}}{Q_{V0}} q_{n_5} \quad (6)$$

144
 146
 165

$$h_{n_5} = \frac{2\Delta H_{V0}}{Q_{V0} - \left(2\Delta H_{V0} \frac{\left[\frac{igA\Delta H_{B0}}{aQ_{B0}} + \frac{igA\Delta H_{B0}}{aQ_{B0}} \cos(2\pi x_B^* m - \pi x_B^*) \right]}{\left[\frac{-ia}{gA} + \frac{2\Delta H_{B0}}{Q_{B0}} \sin(2\pi x_B^* m - \pi x_B^*) \right]} \right)} \quad (9)$$

166
 167
 168
 169

170 where g =gravitational acceleration; a =pipeline wave speed;
 171 A =cross-section pipe area; $i=\sqrt{-1}$; and the variable m =harmonic
 172 peak number in the FRD. For discrete blockages that do not
 173 result in a total constriction of the flow through the pipe, the
 174 term $2\Delta H_{B0}/Q_{B0}$ is small compared to $a/(gA)$ and Eq. (9) sim-
 175 plifies to

$$h_{n_5} = \frac{1}{\frac{1}{2} \left(\frac{\Delta H_{V0}}{Q_{V0}} \right)^{-1} + \left(\frac{a}{gA} \right)^{-2} \left(\frac{\Delta H_{B0}}{Q_{B0}} \right) (1 + \cos(2\pi x_B^* m - \pi x_B^*))} \quad (10)$$

176 Inverting the equation and defining I_B^* as the dimensionless
 177 blockage size, $B=a/gA$ as the pipe characteristic impedance, and
 178 $I_V=\Delta H_{V0}/Q_{V0}$ as the valve impedance gives an expression for the
 179 reciprocal of the peak magnitudes in the FRD as
 180

$$\frac{1}{|h_{n_5}|} = \frac{1}{2I_V} + \frac{I_B^*}{B} (1 + \cos(2\pi x_B^* m - \pi x_B^*)) \quad (11)$$

181 where the frequency of the oscillation (in units of “per peak num-
 182 ber”) in the cosine function is given by x_B^* which is the coefficient

Note that the head perturbation at the upstream reservoir is 145
 zero ($h_{n_1}=0$). An expression for the head perturbation upstream 146
 of the valve based on the elements of the overall transfer matrix, 147
 U , is 148

$$h_{n_5} = \frac{\frac{2\Delta H_{V0}}{Q_{V0}}}{1 - \frac{2\Delta H_{V0}}{Q_{V0}} \frac{U_{11}}{U_{21}}} \quad (7)$$

149

As mentioned previously, the elements of the transfer matrix, U , 150
 can be determined by multiplying the individual matrices for each 151
 hydraulic element together, starting from the downstream bound- 152
 ary. The matrix for pipe sections can be found in Chaudhry 153
 (1987). To isolate the blockage-induced impact on the FRD, these 154
 are considered as frictionless units. The behavior of a discrete 155
 blockage can be considered as similar to an inline valve, and has 156
 the transfer matrix of the form 157

$$\begin{Bmatrix} q \\ h \\ 1 \end{Bmatrix}^{n_3} = \begin{bmatrix} 1 & 0 & 0 \\ -\frac{2\Delta H_{B0}}{Q_{B0}} & 1 & 0 \\ 0 & 0 & 1 \end{bmatrix} \begin{Bmatrix} q \\ h \\ 1 \end{Bmatrix}^{n_2} \quad (8)$$

158

where $Q_{B0}, \Delta H_{B0}$ =steady state flow through the blockage and the 159
 steady state head loss across the blockage, respectively. Formulation 160
 of the overall system transfer matrix and substituting U_{11} and 161
 U_{21} into Eq. (7) gives the frequency response measured at a po- 162
 sition just upstream of the inline valve as 163

to m , and the phase is πx_B^* , given by the remaining term. Eq. (9) 184
 indicates that a blockage induces a sinusoidal oscillation on the 185
 inverted peaks of the FRD. The properties of this blockage- 186
 induced oscillation are as follows: 187

- The frequency of the blockage-induced damping pattern from 188
 Eq. (9) is x_B^* , however, frequency aliasing means that for osc- 189
 illation frequencies greater than the Nyquist frequency of 0.5, 190
 the signals will appear with frequencies of $(1-x_B^*)$. Each ob- 191
 served oscillation frequency in the peaks of the FRD can be 192
 caused by two possible frequencies, one above the Nyquist 193
 frequency and one below, indicating two possible blockage 194
 positions at mirror positions within the pipeline (Lee et al. 195
 2003a). 196
- The phase of the blockage-induced damping pattern is πx_L^* 197
 and is also affected by possible aliasing, where aliased signals 198
 will display a reversed phase, $-\pi x_L^*$. The phase can be used 199
 to indicate whether the frequency underwent aliasing. The sign 200
 of the phase determines the correct blockage position from 201
 the two possible solutions found using the oscillation fre- 202
 quency. Signals with phase located in the first quadrant of the 203
 unit circle ($0 \leq \text{phase} \leq \pi/2$) indicate a blockage in the up- 204

Table 1. Results of Single Blockage Detection

Case	True blockage properties		FRD peak pattern properties			Predicted blockage properties	
	Blockage position, x_B^*	Blockage size, I_B^*	Frequency (1/m)	Phase (rad)	Amplitude ($\times 10^{-5} \text{ m}^2 \text{ s}^{-1}$)	Blockage position, x_B^*	Blockage size, I_B^*
1	0.878	0.062	0.122	-2.711	3.566	0.878	0.062
2	0.366	0.062	0.366	1.120	3.567	0.366	0.062
3	0.831	0.028	0.169	-2.500	1.600	0.831	0.028

205 stream half of the pipe and phases in the third quadrant
 206 $(-\pi/2 \geq \text{phase} \geq -\pi)$ indicate a blockage in the downstream
 207 half.

208 • The amplitude of the block-induced damping pattern is I_B^*/B ,
 209 given in Eq. (9) as the coefficient to the blockage-generated
 210 cosine function, which can be used to determine the blockage
 211 size.

212 The extraction of the frequency, phase, and amplitude of the
 213 blockage-induced pattern from the inverted peaks of the FRD can
 214 be carried out using a Fourier transform, and is illustrated in the
 215 following section. The procedure for blockage detection is as fol-
 216 lows:

- 217 1. Generate the FRD as described in Lee et al. (2005).
- 218 2. Extract the magnitudes of the peaks in the FRD and invert
 219 them.
- 220 3. Perform a Fourier transform of the inverted peak magnitudes
 221 to determine the frequency, phase, and amplitude of the
 222 blockage-induced pattern.
- 223 4. Use the frequency to determine the two possible blockage
 224 locations, then use the value of the phase to determine the
 225 correct location.
- 226 5. Using the amplitude of the oscillation, determine the magni-
 227 tude of the blockage, given by I_B^* .

228 Note that the approximation made between Eq. (9) and Eq. (10)
 229 will generally induce only small errors in the prediction result.
 230 This is evident in Fig. 2 where the pattern created by a large
 231 blockage was shown to be sinusoidal even though the approxima-
 232 tion was violated.

**233 Numerical Validation of Blockage Detection
 234 Technique**

235 The validation of the proposed blockage detection method is
 236 carried out for the pipeline system of Fig. 1. Three individual
 237 cases are considered with the blockage impedances and locations

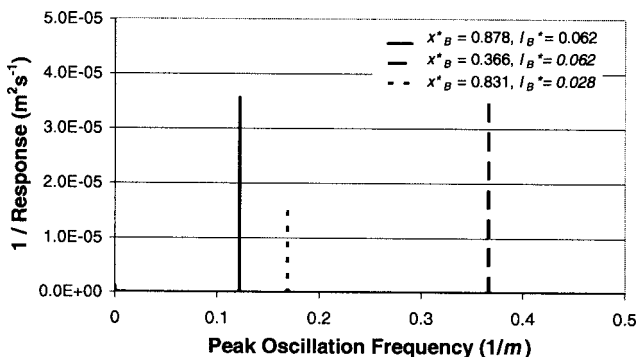


Fig. 3. Spectrum of the inverted peaks magnitudes for three different blockage conditions

as given in Table 1. The head loss across the blockages are 238
 1.15, 1.15, and 0.524 m for Case 1, 2, and 3, respectively, 239
 and the corresponding pipe flows are $1.07 \times 10^{-2} \text{ m}^3 \text{ s}^{-1}$, 240
 $1.07 \times 10^{-2} \text{ m}^3 \text{ s}^{-1}$, and $1.09 \times 10^{-2} \text{ m}^3 \text{ s}^{-1}$. The peaks of the FRD 241
 for each blockage case are first inverted and then a Fourier trans- 242
 form performed, the result of which is shown in Fig. 3. For all 243
 cases, the oscillatory pattern in the inverted peaks has a frequency 244
 corresponding to either x_B^* or $(1-x_B^*)$. For a blockage located in 245
 the first half of the pipeline, the phase is in the first quadrant of 246
 the unit circle and for a blockage in the downstream half of the 247
 pipeline the phase is in the third quadrant. Using the blockage 248
 detection procedure, the blockage is correctly located for all three 249
 cases. The blockage sizes are also correctly determined. Note that 250
 a small discrepancy (approximately 0.5%) exists in the sizing of 251
 the blockage which is not evident in Table 1. This discrepancy is 252
 a result of the approximation made between Eqs. (9) and (10) 253
 which eliminated a small term from the equation, but the impact 254
 of which has no effect on the accuracy of the blockage location. 255

The blockage detection technique can also be expanded to 256
 cater for multiple blockages. In this case, Eq. (9) is rewritten as 257

$$\frac{1}{|h_{n_s}|} = \frac{1}{2I_V} + \frac{I}{B} \sum_{k=1}^{n_{\text{block}}} [I_{B_k}^* (1 + \cos(2\pi x_{B_k}^* m - \pi x_{B_k}^*))] \quad (12) \quad 258$$

where n_{block} = number of blocks in the system. The subscript 259
 k indicates the property is associated with the k th blockage. 260
 Eq. (10) shows that each blockage induces its own oscillatory 261
 pattern on the inverted peaks of the FRD, which can be separated 262
 in the Fourier spectrum as distinct impacts from the different 263
 blockages. This is illustrated in the multiple blockage example 264
 shown in Fig. 4. Two blocks, of size $I_B^* = 0.010$, are located at two 265
 positions simultaneously within the pipeline, the details of which 266
 are shown in Table 2. The Fourier spectrum of the inverted FRD 267
 peaks in Fig. 4 indicates two frequencies, each associated with a 268
 particular blockage within the pipe. Applying the same procedure 269

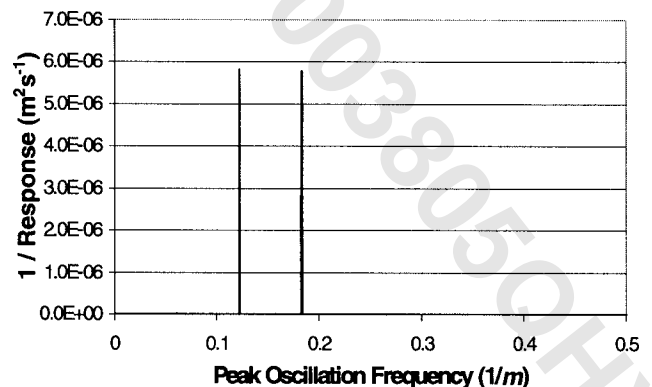


Fig. 4. Spectrum of the inverted peaks magnitudes for a multiple blockage situation

Table 2. Results of Multiple Blockage Detection

	True blockage properties		FRD peak pattern properties			Predicted blockage properties	
	Blockage position, x_B^*	Blockage size, I_B^*	Frequency (1/m)	Phase (rad)	Amplitude ($\times 10^{-5} \text{ m}^2 \text{ s}^{-1}$)	Blockage position, x_B^*	Blockage size, I_B^*
Blockage 1	0.122	0.010	0.122	0.383	0.589	0.122	0.010
Blockage 2	0.183	0.010	0.183	0.575	0.579	0.183	0.010

270 to each oscillation signal gives the correct position and size of
 271 the blocks as shown in Table 2. As in the single blockage case,
 272 excellent accuracy was shown for the location and sizing of the
 273 blockages within the system. Though not evident in Table 2, a
 274 slight error (approximately 1.1%) exists in the predicted blockage
 275 size. The prediction is not as accurate as in the case for a single
 276 blockage and is a result of the approximation made between
 277 Eqs. (9) and (10). Instead of eliminating one small term from the
 278 equation as in the case for a single blockage, the two blockages
 279 resulted in multiple omitted terms and the resultant error is there-
 280 fore slightly greater than the case for a single blockage.

281 Challenges in Real Systems

282 The technique assumes that the behavior of the blockage is simi-
 283 lar to an inline orifice. In reality all blockages can have physical
 284 properties that deviate from this approximation. For example, the
 285 blockage may have a complicated geometry or is distributed
 286 along the length of the pipe. Only in systems where the length of
 287 the pipeline is long compared to the physical size of the blockage
 288 does the response of the blockage approach that of a discrete
 289 blockage, and the proposed technique can be applied to detect and
 290 to locate the problem.

291 The nature of the blockage pattern creates special cases where
 292 the proposed technique will fail. For example, two blockages at
 293 mirror locations in the pipeline will only be detected as one single
 294 blockage. In addition, when the blockage is located close to the
 295 system boundaries or the midpoint of the system, the resultant
 296 oscillation pattern on the peaks of the FRD will have a frequency
 297 close to zero, making the blockage difficult to detect. In these
 298 cases a combination of time domain analysis of the data and the
 299 proposed technique may be necessary to detect and locate the
 300 faults.

301 The application of the technique in a real system will require
 302 additional care with regards to the nature of the transient pertur-
 303 bation. The derivation presented in this paper assumes that the
 304 transient will be created using a side-discharge valve. This
 305 method for generating transients has been performed successfully
 306 in the field by other researchers (Stephens et al. 2005; Stoianov
 307 et al. 2003; Covas et al. 2004). However, the speed of the side-
 308 discharge valve maneuver must be fast to produce a signal that
 309 can excite a large number of modes (FRD peaks) in the system. In
 310 cases where this is not possible, the regression approach pre-
 311 sented in Lee et al. (2004b) may be required to accurately deter-
 312 mine the frequency and phase of the blockage induced pattern.
 313 Note that the proposed technique does not require the transient
 314 signal to be steady oscillatory but the signal must not be so large
 315 in magnitude that it will violate the assumption of linearity. Fur-
 316 ther details concerning the limits to the linearity approximations
 317 can be found in Lee et al. (2003b).

318 In a real pipeline situation the presence of other pipe fittings
 319 will create additional reflections in the transient trace, which in

turn will result in additional oscillations in the FRD. These addi- 320
 tional oscillations may be mistaken as blockages in the system 321
 and careful consultation with construction plans will be necessary 322
 to identify and remove these from the analysis. 323

The derivation presented in this paper assumes that the trans- 324
 ient is generated and measured adjacent to the downstream valve 325
 boundary. Lee et al. (2005) has shown that this is the optimum 326
 system configuration and will lead to the maximum signal to 327
 noise ratio in the measured transient signal. In cases where this 328
 configuration cannot be met, a similar oscillation pattern will still 329
 be evident in the FRD, although the equation describing this pat- 330
 tern will deviate from Eq. (11). A similar approach to the one 331
 presented can be taken to derive the governing equation for these 332
 alternative configurations. 333

Another assumption in the derivation of Eq. (11) is that the 334
 system is frictionless, which may have implications for the techni- 335
 que when it is applied under real conditions. With the aid of 336
 correction procedures for the effects of steady and unsteady fric- 337
 tion, Lee et al. (2004b) have used a similar FRD leak detection 338
 technique (derived with the same frictionless assumption) to ac- 339
 curately locate faults under experimental conditions. It is sus- 340
 pected that the same correction procedures can be used for the 341
 proposed blockage detection technique under real conditions but 342
 this should be verified in future studies. 343

The form of the derived Eq. (11) also provides insight into the 344
 operation of the technique. It is interesting to note that the *fre-* 345
quency of the oscillatory pattern (the coefficient to “*m*” inside the 346
 cosine function) is affected only by the location of the blockage, 347
 x_B^* . The *magnitude* of the oscillatory pattern (the coefficient to the 348
 cosine term) is affected by a number of system parameters includ- 349
 ing the blockage size, wave speed, and the internal diameter. The 350
mean about which the oscillation pattern takes place—the term 351
 that is added to the cosine function, a parameter that plays little 352
 part in the overall blockage detection process—is governed by the 353
 property of the boundary valve. These observations suggest that 354
 the proposed technique may be able to accurately *locate* the 355
 blockage (through an accurate determination of the oscillation 356
 frequency alone) even in a system where the system parameters 357
 (e.g., wave speed, internal diameter, valve characteristics) are not 358
 well known. Note that the technique will not be able to *size* the 359
 blockage under such conditions. A detailed parametric study may 360
 be required in future work to verify this finding. 361

Finally Eq. (11) was derived for a single pipeline system with 362
 specific boundary and system configurations. In the case of a 363
 network, Eq. (11) no longer applies and a similar procedure to the 364
 one presented in this paper will be required to derive the analyti- 365
 cal expression for the blockage induced pattern on the FRD of the 366
 network. However, this approach is ambitious as the resultant 367
 expression will likely to be very complex compared to the form 368
 of Eq. (11) and this expression will also be specific to a particular 369
 network topology. Alternatively, Lee et al. (2005) presented a 370
 method where a complex system can be subdivided into indi- 371
 vidual single pipes and the FRD of each individual pipe seg- 372

373 ment within the network can be extracted. The blockage detection
 374 technique presented in this paper can therefore be applied to the
 375 resultant FRD of each pipe in the network. In order for this ap-
 376 proach to work, a valve must exist at one extremity of the pipe to
 377 create a valve boundary and to partially isolate the pipe from the
 378 remainder of the network. Details of this approach can be found
 379 in Lee et al. (2005).

380 Conclusions

381 A procedure for blockage detection in a single pipeline using the
 382 FRD of the system is presented. A discrete blockage located
 383 within a single pipeline system is shown to generate an oscillatory
 384 pattern in the peaks of the FRD. The frequency, phase, and am-
 385 plitude of this oscillation are related to the blockage location and
 386 size using an analytical expression derived using oscillatory un-
 387 steady flow equations. Once the FRD is extracted from the pipe-
 388 line, the properties of the blockage-induced oscillations can be
 389 determined using a Fourier transform of the inverted peak mag-
 390 nitudes in the FRD. This technique is able to detect, locate, and
 391 size single or multiple discrete blockages. The approximation
 392 used in the derivation of the blockage detection equations was
 393 found to cause a small discrepancy in the estimation of the block-
 394 age size, but did not have any impact on the accuracy of the
 395 blockage location.

396 Notation

397 *The following symbols are used in this paper:*

- 398 A = area of pipeline;
 400 a = wave speed;
 401 B = pipe characteristics impedance $=a/gA$;
 402 C_V = valve loss coefficient;
 403 g = gravitational acceleration;
 404 H = hydraulic grade line elevation or frequency
 405 response function;
 406 h = complex hydraulic grade line perturbation;
 407 $|h|$ = magnitude of head perturbation;
 408 I_B = blockage impedance $=\Delta H_{B0}/Q_{B0}$;
 409 I_B^* = dimensionless blockage size $=I_B/B$;
 410 I_V = valve impedance $=\Delta H_{V0}/Q_{V0}$;
 412 i = imaginary unit, $\sqrt{-1}$;
 413 L = total length of pipeline;
 414 L_A, L_B = lengths of pipe subdivided by the blockage;
 415 m = harmonic peak number;
 416 n_{block} = number of blockages within the pipeline;
 417 Q = discharge;
 418 Q_{B0} = steady state flow through the blockage;
 419 Q_{V0} = steady state flow through the valve;
 420 q = complex discharge perturbation;
 421 t = time;
 422 U = overall transfer matrix for the pipeline system
 423 excluding the boundary valve;
 424 x = distance along pipe;
 425 x_B^* = dimensionless position of blockage $=x_B/L$;
 426 ΔH_{B0} = steady state head loss across the blockage;
 427 ΔH_{V0} = steady state head loss across the valve; and
 428 ω = angular frequency.

References

- Chaudhry, M. H. (1987). *Applied hydraulic transients*, Van Nostrand
 Reinhold, New York. 430
 431
 Covas, D., Ramos, H., Brunone, B., and Young, A. (2004). "Leak detec-
 tion in water trunk mains using transient pressure signals: Field tests
 in Scottish water." *9th Int. Conf. on Pressure Surges*, BHR Group,
 Chester, U.K., 185–198. 432
 433
 434
 435
 De Salis, M. H. F., and Oldham, D. J. (2001). "The development of a
 rapid single spectrum method for determining the blockage character-
 istics of a finite length duct." *J. Sound Vib.*, 243(4), 625–640. 436
 437
 438
 Lee, P., Vítkovský, J., Lambert, M., Simpson, A., and Liggett, J. (2005).
 "Frequency domain analysis for detecting pipeline leaks." *J. Hydraul.
 Eng.*, 131(7), 596–604. 439
 440
 441
 Lee, P. J., and Vítkovský, J. P. (2006). "Discussion of 'Detection of
 partial blockage in single pipelines by P. K. Mohapatra, M. H.
 Chaudhry, A. A. Kassem, and J. Moloo'." *Journal of Hydraulic En-
 gineering*, in press. 442 AQ:
 443 #3
 444
 445
 Lee, P. J., Vítkovský, J. P., Lambert, M. F., Simpson, A. R., and Liggett,
 J. A. (2003a). "Frequency response coding for the location of leaks in
 single pipeline systems." *Int. Conf. on Pumps, Electromechanical De-
 vices and Systems Applied to Urban Water Management*, International
 Association for Hydraulic Research and IHR, Valencia, Spain. 446
 447 AQ:
 448 #4
 449
 450
 Lee, P. J., Vítkovský, J. P., Lambert, M. F., Simpson, A. R., and Liggett,
 J. (2003b). "Discussion of 'Leak detection in pipes by frequency re-
 sponse method using a step excitation by Witness Mpesha, M. H.
 Hanif Chaudhry, and Sarah L. Gassman'." *J. Hydraul. Res.*, 40(1),
 2003, pp. 55–62. 451
 452
 453
 454
 455
 Lee, P. J., Vítkovský, J. P., Lambert, M. F., Simpson, A. R., and Liggett,
 J. A. (2004a). "Detection of leaks in a fluid pipelines using a linear
 system transfer function." *Journal of Hydraulic Engineering*, in press. 456 AQ:
 457 #5
 458
 459
 Lee, P. J., Vítkovský, J. P., Lambert, M. F., Simpson, A. R., and Liggett,
 J. A. (2004b). "Experimental validation of frequency response coding
 for the location of leaks in single pipeline systems." *The practical
 application of surge analysis for design and operation*, *9th Int. Conf.
 on Pressure Surges*, BHR Group, Chester, U.K., 239–253. 460
 461
 462
 463
 Lynn, P. (1982). *An introduction to the analysis and processing of signals*,
 Macmillan, London. 464
 465
 Mermelstein, P. (1967). "Determination of the vocal-tract shape from
 measured formant frequencies." *J. Acoust. Soc. Am.*, 41(5), 1283–
 1294. 466
 467
 468
 Mohapatra, P. K., Chaudhry, M. H., Kassem, A. A., and Moloo, J. (2006).
 "Detection of partial blockage in single pipelines." *J. Hydraul. Eng.*,
 132(2), 200–206. 469
 470
 471
 Schroeder, M. R. (1967). "Determination of the geometry of the human
 vocal tract by acoustic measurements." *J. Acoust. Soc. Am.*, 41,
 1002–1010. 472
 473
 474
 Stephens, M., Simpson, A. R., Lambert, M. F., and Vítkovský, J. P.
 (2005). "Field measurements of unsteady friction effects in a trunk
 transmission pipeline." *7th Annual Symp. on Water Distribution Sys-
 tems Analysis*, ASCE, Anchorage, Alaska. 475
 476
 477
 478
 Stoianov, I., Maksimovic, C., Graham, N., and Dellow, D. (2003). "Field
 validation of the application of hydraulic transients for leak detection
 in transmission pipelines." *Advances in Water Supply Management*,
 CCWI '03, London, 86–97. 479
 480 AQ:
 481 #6
 482
 Vítkovský, J. P., Bergant, A., Lambert, M. F., and Simpson, A. R. (2003).
 "Unsteady friction weighting function determination from transient
 responses." *Pumps, electromechanical devices and systems applied to
 urban water management*, Vol. II, E. Cabrera and E. Cabrera, Jr., eds.,
 Valencia, Spain, 781–789. 483
 484
 485
 486
 487
 Wang, X.-J., Lambert, M. F., and Simpson, A. R. (2005). "Detection and
 location of a partial blockage in a pipeline using damping of fluid
 transients." *J. Water Resour. Plann. Manage.*, 131(3), 244–249. 488
 489
 490
 Wylie, E. B., and Streeter, V. L. (1993). *Fluid transients in systems*,
 Prentice Hall, Englewood Cliffs, N.J. 491
 492